

Superconductivity of Quasi-Two-Dimensional Tight-Binding Electrons in a Strong Magnetic Field

Mitake MIYAZAKI, Keita KISHIGI and Yasumasa HASEGAWA

*Faculty of Science, Himeji Institute of Technology,
Kamigouri-cho, Akou-gun, Hyogo 678-1297, Japan*

(Received)

We have investigated the transition temperature $T_c(H)$ of superconductivity in quasi-two-dimensional (Q2D) tight-binding electrons in a strong magnetic field. When the magnetic field is parallel to 2D conducting plane, $T_c(H)$ of the Q2D superconductor is shown to increase in an oscillatory manner as the magnetic field becomes large and to reach $T_c(0)$ in a strong magnetic field limit for the spin-triplet superconductor. We consider the cases of on-site and nearest sites attractive interaction, and calculate the magnetic field dependences of the transition temperature for various types of symmetry. The first order transition from p_y -wave to p_x -wave is shown to occur at $H \sim 35\text{T}$ when the magnetic field is parallel to the y direction, which will be observed in a triplet superconductor, Sr_2RuO_4 .

KEYWORDS: field-induced superconductivity, organic conductors, quasi-two-dimension, Sr_2RuO_4

§1. introduction

Recently, it has been shown that the quasi-two dimensional (Q2D) superconductivity evolves from the Ginzburg-Landau-Abrikosov-Gor'kov^{1,2)} (GLAG) and Lawrence-Doniach^{3,4,5)} (LD) region to the reentrant phase as a magnetic field becomes large,^{6,7)} which is derived by considering the quantum effect of electron motion in the presence of a strong magnetic field applied parallel to 2D conducting plane. The Q2D systems with layered structure, for example high T_c oxides, β -(BEDT-TTF)₂I₃⁸⁾ and Sr_2RuO_4 ,⁹⁾ have a two-dimensional cylindrical Fermi surface with weak warping along the k_z direction. When the magnetic field H is parallel to the conducting plane, the electrons move in orbits which are the intersection of the Fermi surface and a plane normal to H in a semi-classical picture. Some orbits are open and the others are closed. The former gives a similar effect as Q1D superconductivity in a strong magnetic field.^{10,11,12,13,14)} By neglecting the contribution from the closed orbits, Lebed and Yamaji⁶⁾ calculated the mean field transition temperature of a Q2D superconductor in the parabolic band model and demonstrated the possibility of reentrant superconductivity. In a previous paper,⁷⁾ we calculated the mean field transition temperature

numerically by taking account of the eigenstates of three-dimensional tight-binding electrons in a strong magnetic field. In this formulation, we can treat Q1D and Q2D in the same manner by changing t_b/t_a , where t_a and t_b are hopping matrix elements in the conducting plane. In the previous calculation,⁷⁾ however, we considered only on-site attractive interaction for the Q2D systems.

The high T_c oxides are thought to be Q2D d -wave superconductors and κ -(BEDT-TTF)₂Cu[N(CN)₂]Br^{15,16,17,18)} is shown to be anisotropic Q2D with line nodes of the gap. Rice and Sigrist¹⁹⁾ proposed that Sr₂RuO₄ could be a spin-triplet superconductor by analogy with ³He and experimental evidences for the triplet superconductivity have been observed.^{20,21,22)} The Q2D anisotropic superconductivity in a strong magnetic field is of great interest.

In this paper, we assume the nearest site attractive interaction in tight-binding model, and we examine the transition temperature of anisotropic superconducting states in a strong magnetic field.

§2. Model and Green Function of Tight-Binding Electrons in a Magnetic Field

The tight-binding electrons in a magnetic field are described by the Hamiltonian (we take \hbar , k_B and the velocity of light to be 1),

$$\begin{aligned} \mathcal{H} &= \mathcal{H}_0 + \mathcal{H}_U \\ \mathcal{H}_0 &= -t_a \sum_{(i,j)_{a,\sigma}} e^{i\theta_{ij}} c_{i,\sigma}^\dagger c_{j,\sigma} - t_b \sum_{(i,j)_{b,\sigma}} e^{i\theta_{ij}} c_{i,\sigma}^\dagger c_{j,\sigma} \\ &\quad - t_c \sum_{(i,j)_{c,\sigma}} e^{i\theta_{ij}} c_{i,\sigma}^\dagger c_{j,\sigma} - \mu \sum_{i,\sigma} c_{i,\sigma}^\dagger c_{i,\sigma} \\ &\quad - \sum_{i,\sigma} \sigma \mu_B H c_{i,\sigma}^\dagger c_{i,\sigma} \end{aligned} \quad (1)$$

$$\mathcal{H}_U = \sum_{\langle i,j \rangle, \sigma, \sigma'} U_{ij} c_{i,\sigma}^\dagger c_{i,\sigma} c_{j,\sigma'}^\dagger c_{j,\sigma'}, \quad (2)$$

where $c_{i,\sigma}^\dagger$ and $c_{i,\sigma}$ are creation and annihilation operators at the i site, μ is the chemical potential, $\sigma \mu_B H$ is the Zeeman energy for \uparrow (\downarrow) spin ($\sigma = +(-)$), U_{ij} is the interaction between electrons at i and j sites and

$$\theta_{ij} = \frac{2\pi}{\phi_0} \int_i^j \mathbf{A} dl. \quad (3)$$

In the above, \mathbf{A} is the vector potential and ϕ_0 is the flux quantum. We consider the Q2D system with the hopping matrix elements $t_a \geq t_b \gg t_c$. The interlayer hopping matrix element t_c is taken to be larger than transition temperature T_c for $H = 0$, so that the fluctuation due to the low dimension is small and we take the mean field approximation in this paper.

In the interaction Hamiltonian, eq.(2), we take the on-site interaction and nearest-site interaction

along each axis as

$$U_{ij} = \begin{cases} U_0 & \text{if } \mathbf{r}_i = \mathbf{r}_j \\ U_\delta & \text{if } \mathbf{r}_i = \mathbf{r}_j \pm \hat{\boldsymbol{\delta}} \\ 0 & \text{otherwise} \end{cases} . \quad (4)$$

where $\hat{\boldsymbol{\delta}} = \hat{\mathbf{x}}, \hat{\mathbf{y}}$ and $\hat{\mathbf{z}}$ are unit vectors along a axis, b axis and c axis, respectively. The Fourier-transform of the interaction is obtained as

$$U(\mathbf{q}) = U_0 + 2U_x \cos(aq_x) + 2U_y \cos(bq_y) + 2U_z \cos(cq_z). \quad (5)$$

In this paper, the magnetic field H is parallel to the b axis. We use the vector potential $\mathbf{A} = (0, 0, -Hx)$. Since the magnetic field considered in this paper is not extremely strong ($\phi/\phi_0 \ll 1$, where $\phi = Hac$ is flux per unit cell), the change of the electron number as a function of H may be very small in Q1D and Q2D case. This can be understood by noting that there are no closed orbits in the Q1D case and only small part of the orbits are closed in the Q2D case in the semi-classical picture. Therefore, the chemical potential μ is fixed for given t_a, t_b and t_c to give a quarter-filled band at $H = 0$ instead of electron number to be fixed.

The noninteracting Hamiltonian is written as

$$\mathcal{H}_0 = \sum_{\sigma, \mathbf{k}} C_\sigma^\dagger \begin{pmatrix} \ddots & & & & V^* \\ & M_{-1} & V & 0 & \\ & V^* & M_0 & V & \\ & 0 & V^* & M_1 & \\ V & & & & \ddots \end{pmatrix} C_\sigma, \quad (6)$$

where

$$M_n = -2t_a \cos[a(k_x + nG)] - 2t_b \cos(bk_y) - \sigma \mu_B H - \mu, \quad (7)$$

$$V = -t_c e^{ick_z}, \quad (8)$$

$$C_\sigma^\dagger = (\dots, c_\sigma^\dagger(\mathbf{k} - \mathbf{G}), c_\sigma^\dagger(\mathbf{k}), c_\sigma^\dagger(\mathbf{k} + \mathbf{G}), \dots), \quad (9)$$

$$\mathbf{G} = (G, 0, 0) = \left(\frac{2\pi}{a} \frac{\phi}{\phi_0}, 0, 0 \right). \quad (10)$$

The size of the matrix in eq.(6) is $q \times q$ if $\phi/\phi_0 = p/q$, where p and q are mutually prime integers and infinite if ϕ/ϕ_0 is irrational. The summation in \mathbf{k} should be done in a magnetic Brillouin zone, $|k_x| < \pi/(qa)$, $|k_y| < \pi/b$, and $|k_z| < \pi/c$. The eigenvalues of the matrix in eq.(6) for fixed k_y

have very rich structure as a function of the magnetic field if $t_c \sim t_a$ as shown by Hofstadter.²⁴⁾ In the case of $t_c \ll t_a$, which is the case for Q1D and Q2D systems, however, the energy is almost continuous except for the large gaps near the bottom and top of the energy. The gaps near the bottom and the top can be interpreted as the result of the Landau quantization in the closed orbit and the negligible gaps can be understood as the small probability of the magnetic breakdown in the open orbit. Since we consider the instability to the superconductivity, only the states near the Fermi surface with the energy $|\epsilon - \mu| < T$ are important. For the electrons of less-than-half filled band, or the quarter-filled electrons, we can consider only the part of the matrix in eq.(6) which has, for example, $|a(k_x + nG)| < (3/4)(\pi/a)$. By this approximation ϕ/ϕ_0 is not restricted to be a rational number. The Brillouin zone should be taken as $|k_x| < G/2$ instead of the magnetic Brillouin zone $|k_x| < \pi/(qa) = G/(2p)$ for the rational magnetic field case ($\phi/\phi_0 = p/q$). The energy does not depend on k_z in this approximation. This can be seen by changing $c_\sigma^\dagger(\mathbf{k} + m\mathbf{G})$ to $e^{-imck_z} c_\sigma^\dagger(\mathbf{k} + m\mathbf{G})$, by which only $(1, q)$ and $(q, 1)$ elements in eq.(6) depend on k_z but they are irrelevant for the energy near the Fermi level in the case of $t_c \ll t_a$. The effects of the closed orbits and the magnetic breakdown are taken into account correctly in this approximation as shown in Fig. 1.

We get the energy

$$\varepsilon_{n, \mathbf{k}, \sigma} = \epsilon(n, k_x) - 2t_b \cos(bk_y) - \sigma\mu_B H - \mu \quad (11)$$

and the eigenstates $|\Psi_\sigma(n, \mathbf{k})\rangle$ by numerically diagonalizing the matrix of size of the order of $[(3/4) \cdot 2\pi/G] \times [(3/4) \cdot 2\pi/G]$.

The creation operators $c_\sigma^\dagger(\mathbf{k} + m\mathbf{G})$ is expressed by the creation operators of the eigenstates ($\Psi_\sigma^\dagger(n, \mathbf{k})$) as

$$c_\sigma^\dagger(\mathbf{k} + m\mathbf{G}) = e^{imck_z} \sum_n \phi_{k_x}^*(m, n) \Psi_\sigma^\dagger(n, \mathbf{k}), \quad (12)$$

where the coefficient $\phi_{k_x}(m, n)$ can be calculated numerically. Notice that $\phi_{k_x}(m, n)$ does not depend on k_y and k_z .

The real space Green's function is given by

$$\begin{aligned} G_\sigma(\mathbf{r}_i, \mathbf{r}'_j, i\omega_l) &= - \int_0^\beta d\tau e^{i\omega_l \tau} \left\langle T_\tau C_{\mathbf{r}_i, \sigma}(\tau) C_{\mathbf{r}'_j, \sigma}^\dagger(0) \right\rangle \\ &= \sum_{\mathbf{k}, n} \sum_{m, m'} \frac{\phi_{k_x}(m, n) \phi_{k_x}^*(m', n)}{i\omega_l - \varepsilon_{n, \mathbf{k}, \sigma}} \\ &\quad \times e^{i(\mathbf{r}'_j - \mathbf{r}_i) \cdot \mathbf{k} + i(m' \mathbf{r}'_j - m \mathbf{r}_i) \cdot \mathbf{G}} \\ &\quad \times e^{i(m' - m)ck_z}, \end{aligned} \quad (13)$$

where $\omega_l = (2l + 1)\pi T$ is the Matsubara frequency.

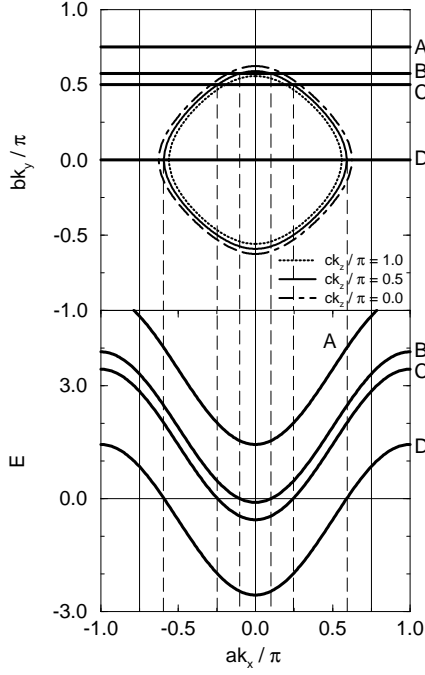


Fig. 1. Fermi surface in k_x - k_y plane and energy as a function of k_x in Q2D. Three curves in the upper figure are the Fermi surface in the planes of $k_z = \pi/c$, $\pi/(2c)$ and 0, respectively. The lower figure shows the energy as a function of k_x for four values of k_y shown in the upper figure, representing no-orbit (A), closed orbit (B) and two open orbits (C) and (D) from the top. We neglect the region of $|ak_x/\pi| > 3/4$. In the presence of magnetic field gaps open at $k_x = mG/2$ with integer $m \neq 0$.

The linearized gap equation for isotropic and anisotropic pairing in coordinate representation is obtained in the mean field approximation as

$$\Delta_{\sigma\sigma'}(\mathbf{r}_i, \mathbf{r}_j) = U_{ij} \sum_s \sum_t K_{\sigma\sigma'}(\mathbf{r}_i, \mathbf{r}_j; \mathbf{r}'_s, \mathbf{r}'_t) \Delta_{\sigma\sigma'}(\mathbf{r}'_s, \mathbf{r}'_t), \quad (14)$$

where

$$K_{\sigma\sigma'}(\mathbf{r}_i, \mathbf{r}_j; \mathbf{r}'_s, \mathbf{r}'_t) \equiv T \sum_{\omega_l} G_{\sigma}(\mathbf{r}_i, \mathbf{r}'_s, i\omega_l) G_{\sigma'}(\mathbf{r}_j, \mathbf{r}'_t, -i\omega_l). \quad (15)$$

§3. Spin-triplet superconductivity

In this section, we consider the spin-triplet superconductivity. We consider only the equal-spin-pairing state in the following. The Zeeman effect does not play any important role in a strong magnetic field, as long as we neglect a change of the density of states of the up and down spin.

For the spin-triplet case, we define “ p_δ -wave” the order parameter as

$$\Delta_{\uparrow\uparrow}^{p_\delta}(\mathbf{r}) \equiv \frac{1}{2} \left[\Delta_{\uparrow\uparrow}(\mathbf{r}, \mathbf{r} + \hat{\boldsymbol{\delta}}) - \Delta_{\uparrow\uparrow}(\mathbf{r} + \hat{\boldsymbol{\delta}}, \mathbf{r}) \right]. \quad (16)$$

Here, the Fourier transformation of the order parameters is defined by

$$\Delta_{N\uparrow\uparrow}^{p_\delta}(\mathbf{q}) = \int d\mathbf{r} \Delta_{\uparrow\uparrow}^{p_\delta}(\mathbf{r}) e^{-i(\mathbf{q} + N\mathbf{G}) \cdot (\mathbf{r} + \hat{\boldsymbol{\delta}}/2)}, \quad (17)$$

and

$$\Delta_{\uparrow\uparrow}^{p\delta}(\mathbf{r}) = \sum_{\mathbf{q}, N} e^{i(\mathbf{q}+N\mathbf{G})\cdot(\mathbf{r}+\hat{\boldsymbol{\delta}}/2)} \Delta_N^{p\delta}(\mathbf{q}), \quad (18)$$

where q_x is taken as $-G/2 < q_x \leq G/2$ and N is integer. The p_δ -wave state can be a solution of eq. (14) if $U_\delta < 0$. When the system has tetragonal symmetry, p_x and p_y have the same coupling constant at $H = 0$ and $p_x + ip_y$ will be stabilized at $T < T_c$, resulting in the nodeless gap in the Fermi surface. The magnetic field along the b axis lifts the degeneracy of p_x and p_y even in a weak magnetic field as discussed by Agterberg²³⁾ in the GL theory.

The linearized gap equation, eq.(14), is written as a matrix equation for $\Delta_N^{d\delta}(\mathbf{q})$. The transition temperature is obtained by the condition that the nontrivial solution exists. It can be shown that the maximum transition temperature is obtained for $\mathbf{q} = 0$. The matrix equation is reduced to the equations for even N and odd N . For even N the linearized gap equation is obtained as

$$\begin{aligned} \Delta_{2l\uparrow\uparrow}^{\mathcal{T}} &= U_\delta T \sum_{k_x k_y} \sum_{l' n n'} \sum_{\omega_l} \frac{1}{i\omega_l - \varepsilon_{n, k_x, k_y \uparrow}} \frac{-1}{i\omega_l + \varepsilon_{n', -k_x, -k_y \uparrow}} \\ &\times \sum_{m_1 m_2} \sum_{m_3 m_4} \delta_{m_1 - m_2, m_3 - m_4} \delta_{m_1 + m_3, -N} \delta_{m_4 - m_3, \frac{N}{2} - \frac{N'}{2}} \\ &\times \phi_{k_x}(m_1, n) \phi_{k_x}(m_2, n) \phi_{-k_x}(m_3, n') \phi_{-k_x}(m_4, n') \\ &\times \left[\cos \left\{ \left(m_4 - m_3 - \frac{N}{2} + \frac{N'}{2} \right) \mathbf{G} \cdot \hat{\boldsymbol{\delta}} \right\} \right. \\ &\left. - \cos \left\{ 2k_\delta + \left(m_4 + m_3 + \frac{N}{2} + \frac{N'}{2} \right) \mathbf{G} \cdot \hat{\boldsymbol{\delta}} \right\} \right] \Delta_{2l\uparrow\uparrow}^{\mathcal{T}} \\ &= U_\delta \sum_{l'} \Pi_{2l, 2l'}^{\mathcal{T}} \Delta_{2l'\uparrow\uparrow}^{\mathcal{T}}, \end{aligned} \quad (19)$$

where

$$\begin{aligned} \Pi_{2l, 2l'}^{\mathcal{T}}(q_x) &= \sum_{k_x, k_y} \sum_{n, n'} \sum_m (\gamma_{\mathbf{k}m}^{\mathcal{T}})^2 \\ &\times \phi_{k_x}(m - l, n) \phi_{k_x}(m - l', n) \\ &\times \phi_{-k_x}(-m - l, n') \phi_{-k_x}(-m - l', n') \\ &\times \frac{1 - f(\varepsilon_{n, k_x, k_y \uparrow}) - f(\varepsilon_{n', -k_x - q_x, -k_y \uparrow})}{2(\varepsilon_{n, k_x, k_y \uparrow} + \varepsilon_{n', -k_x - q_x, -k_y \uparrow})}, \end{aligned} \quad (20)$$

where $f(\varepsilon)$ is the Fermi distribution function and $\gamma_{\mathbf{k}m}^{\mathcal{T}}$ has the following forms for each order parameter:

$$\gamma_{\mathbf{k}m}^{\mathcal{T}} = \begin{cases} \sin[a(k_x - mG)] & \mathcal{T} = p_x\text{-wave} \\ \sin(bk_y) & \mathcal{T} = p_y\text{-wave} \\ \sin(ck_z) & \mathcal{T} = p_z\text{-wave} \end{cases} . \quad (21)$$

For odd N , we get

$$\Delta_{2l+1\uparrow\uparrow}^{\mathcal{T}} = U_\delta \sum_{l'} \Pi_{2l+1, 2l'+1}^{\mathcal{T}} \Delta_{2l'+1\uparrow\uparrow}^{\mathcal{T}}, \quad (22)$$

where

$$\begin{aligned}
\Pi_{2l+1,2l'+1}^T(q_x) &= \sum_{k_x, k_y} \sum_{n, n'} \sum_m (\gamma_{\mathbf{k}m}^T)^2 \\
&\times \phi_{k_x}(m-l, n) \phi_{k_x}(m-l', n) \\
&\times \phi_{-k_x}(-m-l-1, n') \phi_{-k_x}(-m-l'-1, n') \\
&\times \frac{1 - f(\varepsilon_{n, k_x, k_y}) - f(\varepsilon_{n', -k_x - q_x, -k_y})}{2(\varepsilon_{n, k_x, k_y} + \varepsilon_{n', -k_x - q_x, -k_y})}.
\end{aligned} \tag{23}$$

The transition line is given by $1 - gU_\delta = 0$, where g is the maximum eigenvalue of the matrix Π for even and odd N . In this paper, we calculate the field dependence of g at low temperature instead of calculating the transition temperature.

In the following, we consider the Q2D superconductor of the quarter-filled electrons with parameters $t_b/t_a = 1$, $t_c/t_a = 0.05$ and $T/t_a = 0.001$. In Fig. 2, we plot the effective coupling constant g/g_0 for each states as a function of $aG/(2\pi) = \phi/\phi_0$, where g_0 is the effective coupling constant for $t_c = 0$, which corresponds to that in the absence of magnetic field. For example, the magnetic field of 20 Tesla corresponds to $\phi/\phi_0 \simeq 0.0036$ for $a = 3.87\text{\AA}$ and $c = 12.7\text{\AA}$ (Sr_2RuO_4). It is found that g/g_0 obtained by diagonalizing the even part of the matrix Π increases in an oscillatory manner as a magnetic field becomes larger and reaches that in the absence of magnetic field, while g/g_0 for the odd part becomes zero in the strong field limit. In the semi-classical treatment of the magnetic field, superconductivity is destroyed in a strong magnetic field, since the energies of electrons with wave numbers \mathbf{k} and $-\mathbf{k}$ is not equal. However, as is seen in eq. (19), the instability to the superconductivity is caused by the pairs between the states (n, \mathbf{k}) and $(n', -\mathbf{k})$ with the same energy $\varepsilon_{n, k_x, k_y} = \varepsilon_{n', -k_x, -k_y}$. On the other hands, the coefficient $\phi_{k_x}(m, n)$ becomes small in a weak magnetic field region but a lot of states within the energy range of T contribute to forming Cooper pairs, which will reproduce the GLAG result.

We obtain g/g_0 is larger in the p_x -wave state than in the p_y -wave state for $\phi/\phi_0 \geq 0.0065$ as shown in Fig. 2. The difference of g/g_0 can be understood as follows. Since the electron orbit at $k_y \approx 0$ is open, we can use the linearized dispersion and we can treat it as a quasi-one dimensional system.⁷⁾ Then we obtain $\phi_{k_x}(m, n) \approx J_{m-n}(2t_c/v_F(k_y)G)$, where J is the Bessel function and $v_F(k_y)$ is the k_y -dependent k_x component of the Fermi velocity.⁷⁾ Therefore, for the larger $v_F(k_y)$, the larger effect of the magnetic field is expected. On the other hand, the electron orbit at $k_y \approx \pi/2b$ in the quarter filled band is closed or has a small $v_F(k_y)$ even if the orbit is open (see Fig. 1). In the p_x -wave state the amplitude of the order parameter is largest at $k_x = \pi/2a$, which corresponds to $k_y \approx 0$ in the Fermi surface of the quarter filled band. The order parameter in p_y -wave state is zero at $k_y = 0$. Thus the quantum effect, which causes the increase of g/g_0 in a strong magnetic field, is larger in the p_x -wave state than that in the p_y -wave state. This is a simple interpretation using

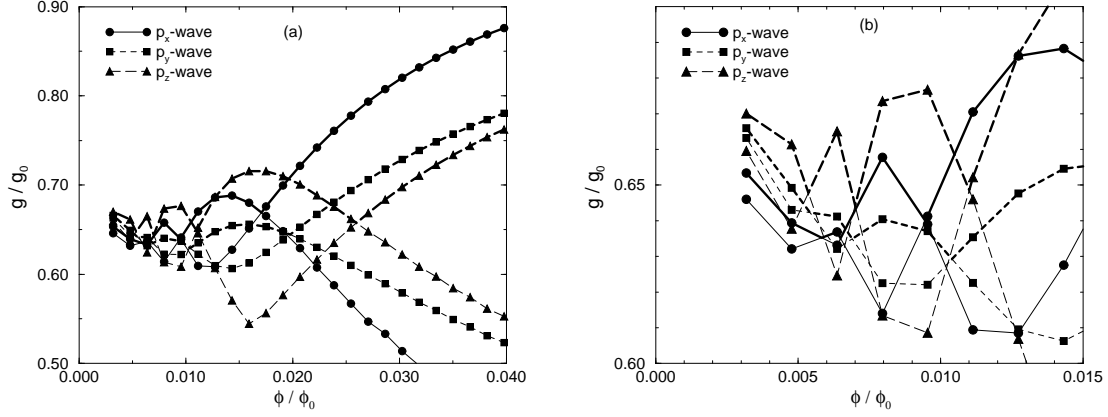


Fig. 2. (a) Effective coupling constant as a function of ϕ/ϕ_0 in the case of $t_b/t_a = 1.0$, $t_c/t_a = 0.05$, $T/t_a = 0.001$ and $\mathbf{H} \parallel y$. Two lines for each state are obtained from the even and odd parts. The larger g/g_0 are shown by thick lines. (b) The low field region.

the Fermi surface in $H = 0$. In the case of $H \neq 0$, we can interpret in the same way as follows. By using the approximation of the linearized dispersion, we can write eq. (20) for the p_x and p_y wave as,

$$\begin{aligned}
\Pi_{2l,2l'}^{\mathcal{T}} &= \sum_{k_x, k_y} \left\{ \frac{\sin^2 a(k_x - k_F(k_y))}{\sin^2 b k_y} \right\} \sum_N \\
&\times \frac{1 - f(v_F(k_y)(k_x - k_F(k_y))) - f(v_F(k_y)(k_x + NG - k_F(k_y)))}{v_F(k_y)(2k_x + NG - 2k_F(k_y))} \\
&\times \int d\theta J_{N-2l} \left(\frac{2t_c}{v_F(k_y)G} \sin \theta \right) J_{N-2l'} \left(\frac{2t_c}{v_F(k_y)G} \sin \theta \right), \quad (24)
\end{aligned}$$

where $k_F(k_y)$ is the k_y -dependent Fermi wave number. The large contribution comes from the region of large $v_F(k_y)$, i.e. $k_y \approx 0$, where $\sin^2 a(k_x - k_F(k_y)) > \sin^2 b k_y$. As a result, the g/g_0 for p_x -wave is larger than that for p_y -wave. In the tetragonal system with $t_a = t_b \gg t_c$ and $U_x = U_y \gg U_z$, the p_x state is realized at the transition line in the strong magnetic field along the b axis (y direction), and the p_y component will become finite at the second transition at lower temperature.

In the weak magnetic field, we can apply the GL theory. As shown by Agterberg,²³⁾ only the p_y -wave orders at H_{c2} (or at the transition temperature $T_c(H)$) when H is along the b axis, and at the second transition the p_x -wave becomes finite. The difference of the transitions for the p_x - and p_y -waves comes from the difference of the GL parameters κ_1 and κ_2 ($\kappa_1 > \kappa_2$), which are the

coefficients of the gradient terms ($|D_x\Delta_{\uparrow\uparrow}^{p_x}(\mathbf{r})|^2 + |D_y\Delta_{\uparrow\uparrow}^{p_y}(\mathbf{r})|^2$) and ($|D_y\Delta_{\uparrow\uparrow}^{p_x}(\mathbf{r})|^2 + |D_x\Delta_{\uparrow\uparrow}^{p_y}(\mathbf{r})|^2$), respectively, where $D_i = \nabla_i - eA_i$.

At a first glance, the GL theory and our result obtained in the strong field may be considered to be incompatible, but it is reasonable. As discussed above the quantum effect of the magnetic field to increase g/g_0 in a strong magnetic field is stronger in the p_x -wave than in the p_y -wave for $H \parallel b$. In the same way the orbital frustration effect to reduce the transition temperature in a weak magnetic field is stronger in the p_x -wave than in the p_y -wave, resulting in the lower transition temperature in the p_x -wave in a weak magnetic field. In the crossover region of the magnetic field relative value of g/g_0 for the p_x -wave and the p_y -wave will change. In Fig. 2(b), we see these features at $\phi/\phi_0 \approx 0.0065$ ($H \sim 35\text{T}$).

§4. Spin-singlet superconductivity

In this section, we consider the spin-singlet superconductivity. In the presence of the nearest-site interaction, $\Delta_{\uparrow\downarrow}(\mathbf{r}, \mathbf{r} + \hat{\delta}) = -\Delta_{\downarrow\uparrow}(\mathbf{r}, \mathbf{r} + \hat{\delta}) = \Delta_{\uparrow\downarrow}(\mathbf{r} + \hat{\delta}, \mathbf{r}) = -\Delta_{\downarrow\uparrow}(\mathbf{r} + \hat{\delta}, \mathbf{r})$. Therefore, the order parameters of “ d_δ -wave” is defined by

$$\Delta_{\uparrow\downarrow}^{d_\delta}(\mathbf{r}) \equiv \frac{1}{2}[\Delta_{\uparrow\downarrow}(\mathbf{r}, \mathbf{r} + \hat{\delta}) + \Delta_{\uparrow\downarrow}(\mathbf{r} + \hat{\delta}, \mathbf{r})] \quad (25)$$

The d_x -wave or d_y -wave is realized only if $U_x < 0$ and $U_0 = 0$ or $U_y < 0$ and $U_0 = 0$, respectively. In contrast to the spin-triplet superconductivity, if $U_0 \neq 0$, d_x and d_y are not self-consistent solutions of eq. (14) but the linear combination of $\Delta_{\uparrow\downarrow}^{d_x}(r)$, $\Delta_{\uparrow\downarrow}^{d_y}(r)$ and $\Delta_{\uparrow\downarrow}^s \equiv \Delta_{\uparrow\downarrow}(r, r)$ can be a self-consistent solution. If the system has a tetragonal symmetry ($t_a = t_b$ and $U_x = U_y < 0$), the d -wave ($d_x - d_y$) is realized at $H = 0$. However, $d_x - d_y$ is not the self-consistent solution in the presence of the magnetic field along the b axis. The d_z is realized as long as $U_z < 0$ and the higher terms in t_c/t_a are neglected. In this section we consider the case that one of the interactions (U_0 or U_δ) is negative and the others are zero, so that s or d_δ -wave is realized, for simplicity. Here, we write

$$\Delta_{\uparrow\downarrow}^{d_\delta}(\mathbf{r}) = \sum_{\mathbf{q}, N} e^{i(\mathbf{q} + N\mathbf{G}) \cdot (\mathbf{r}_i + \hat{\delta}/2)} \Delta_{N\uparrow\downarrow}^{d_\delta}(\mathbf{q}). \quad (26)$$

By taking $\hat{\delta} = 0$, we get the s -wave order parameter.

The linearized gap equation is written as a matrix equation for $\Delta_{N\uparrow\downarrow}^{d_\delta}(\mathbf{q})$ as in the spin-triplet case. The matrix equation is separated into even N and odd N parts. We get

$$\Delta_{2l\uparrow\downarrow}^S = \lambda \sum_{l'} \Pi_{2l, 2l'\uparrow\downarrow}^S \Delta_{2l'\uparrow\downarrow}^S, \quad (27)$$

where coupling constant λ is U_0 or U_δ and

$$\begin{aligned} \Pi_{2l, 2l'}^S &= \sum_{k_x, k_y} \sum_{n, n'} \sum_m (\gamma_{\mathbf{k}m}^S)^2 \\ &\times \phi_{k_x}(m - l, n) \phi_{k_x}(m - l', n) \end{aligned}$$

$$\begin{aligned} & \times \phi_{-k_x}(-m-l, n') \phi_{-k_x}(-m-l', n') \\ & \times \frac{1 - f(\varepsilon_{n, k_x, k_y, \uparrow}) - f(\varepsilon_{n', -k_x, -k_y, \downarrow})}{2(\varepsilon_{n, k_x, k_y, \uparrow} + \varepsilon_{n', -k_x, -k_y, \downarrow})}, \end{aligned} \quad (28)$$

where $\gamma_{\mathbf{k}m}^{\mathcal{S}}$ has the following forms for each order parameter:

$$\gamma_{\mathbf{k}m}^{\mathcal{S}} = \begin{cases} 1 & \mathcal{S}=s\text{-wave} \\ \cos[a(k_x - mG)] & \mathcal{S}=d_x\text{-wave} \\ \cos(bk_y) & \mathcal{S}=d_y\text{-wave} \\ \cos(ck_z) & \mathcal{S}=d_z\text{-wave} \end{cases} . \quad (29)$$

For odd N , we get

$$\Delta_{2l+1\uparrow\downarrow}^{\mathcal{S}} = \lambda \sum_{l'} \Pi_{2l+1, 2l'+1\uparrow\downarrow}^{\mathcal{S}} \Delta_{2l'+1\uparrow\downarrow}^{\mathcal{S}}, \quad (30)$$

where

$$\begin{aligned} \Pi_{2l+1, 2l'+1}^{\mathcal{S}} &= \sum_{k_x, k_y} \sum_{n, n'} \sum_m (\gamma_{\mathbf{k}m}^{\mathcal{S}})^2 \\ & \times \phi_{k_x}(m-l, n) \phi_{k_x}(m-l', n) \\ & \times \phi_{-k_x}(-m-l-1, n') \phi_{-k_x}(-m-l'-1, n') \\ & \times \frac{1 - f(\varepsilon_{n, k_x, k_y, \uparrow}) - f(\varepsilon_{n', -k_x, -k_y, \downarrow})}{2(\varepsilon_{n, k_x, k_y, \uparrow} + \varepsilon_{n', -k_x, -k_y, \downarrow})}. \end{aligned} \quad (31)$$

In the following, we neglect the Zeeman energy for simplicity to show the different behavior between each state obviously. We first calculate the effective coupling constant of s -wave superconductivity in a strong magnetic field and examine its t_c/t_a dependence.

In Fig. 3, we plot the effective coupling constant as a function of ϕ/ϕ_0 . The effective coupling constant reaches that for $t_c = 0$ as a magnetic field increases. We find that the effective coupling constant depends strongly on the hopping matrix elements between layers t_c . As t_c/t_a becomes small, the oscillation of g/g_0 becomes small, and the value of g/g_0 increases in whole. Thus, reentrant behavior will be observed in weaker magnetic field in the superconductor with smaller t_c/t_a .

We now study the effective coupling constant of Q2D anisotropic superconductor with $t_c/t_a = 0.05$. In Fig. 4, we plot g/g_0 obtained by each pairing state as a function of ϕ/ϕ_0 .

For each order parameter, g/g_0 of the even part increases and that of the odd part decreases in a strong magnetic field limit. The effective coupling constant g/g_0 in the d_y -wave state is larger than that in the d_x -wave state. This can be understood as in the spin-triplet case. The d_y -wave have a largest order parameter at $k_y = 0$ and its order parameter is zero at $k_y = \pi/2b$, while the order parameter of the d_x -wave is largest at $k_x = 0$ ($k_y \approx \pi/2b$ for the quarter filled band) and

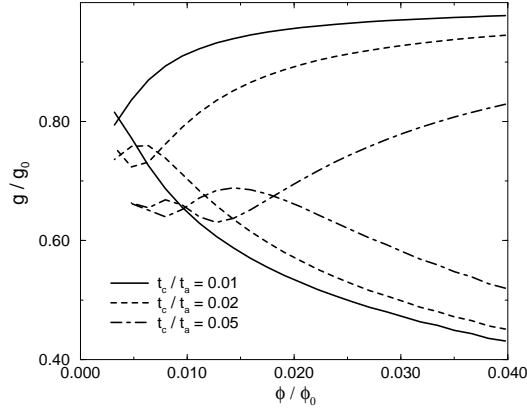


Fig. 3. Effective coupling constant of the s-wave pairing as a function of ϕ/ϕ_0 in the case of $t_b/t_a = 1.0$, $T/t_a = 0.001$ and $\mathbf{H} \parallel y$.

zero at $k_x = \pi/2a$ ($k_y \approx 0$). As a result, the recovery of g/g_0 in the strong magnetic field due to the quantum effect in the open orbit occurs in lower magnetic field for the d_y state than for the d_x state as seen in Fig. 4(b).

§5. Conclusion

In this paper we study the anisotropic superconductivity of tight-binding electrons with hopping matrix elements $t_a = t_b \gg t_c$ as a function of the magnetic field parallel to the b axis. We calculate the energies and the eigenstates in the magnetic field by numerically diagonalizing the matrix and the effective coupling constant is calculated by using these values. The effects of both open and closed orbits are taken into account in our calculation. We consider the attractive interaction between electrons in the nearest sites along each axis to realize the anisotropic superconductivity. With these interactions singlet (d_x , d_y and d_z) and triplet (p_x , p_y and p_z) superconductivities are possible. The effective coupling constant, g/g_0 , for these anisotropic superconductivities are calculated. It is obtained that g/g_0 approaches to 1 as H becomes large and it depends on the symmetry of the order parameter. As shown in Figs. 2 and 4, we find that the p_x -wave (d_y -wave) state gives higher transition temperature than that of p_y -wave (d_x -wave) in the strong magnetic field region, and both of them reach the transition temperature of zero magnetic field in a strong field limit. The first order transition from p_y -wave to p_x -wave is predicted at $H \sim 35\text{T}$, which will be observed in the p -wave superconductor, Sr_2RuO_2 .

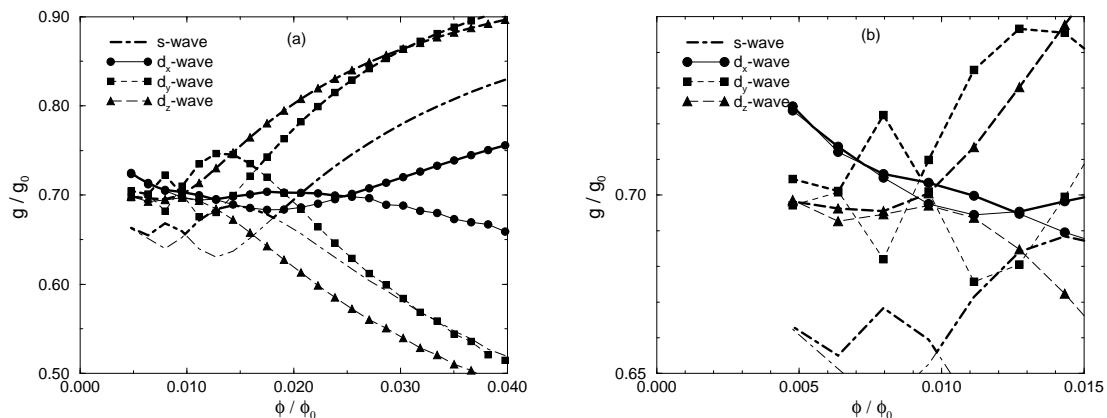


Fig. 4. (a) Effective coupling constant as a function of ϕ/ϕ_0 in the case of $t_b/t_a = 1.0$, $t_c/t_a = 0.05$, $T/t_a = 0.001$ and $\mathbf{H} \parallel y$. Two lines for each state are obtained from the even and odd parts. The larger g/g_0 are shown by thick lines. (b) The low field region.

§6. Acknowledgment

One of the authors (Y. H) thank D. F. Agterberg and Z. Q. Mao for useful discussions. This work was partially supported by Grant-in-Aid for JSPS Fellows from the Ministry of Education, Science, Sports and Culture. One of the authors (K. K) was financially supported by the Research Fellowships of the Japan Society for the Promotion of Science for Young Scientists.

References

-
- [1] A. A. Abrikosov: Zh. Eksp. Teor. Fiz. **32** (1957) 1442.
 - [2] L. P. Gor'kov: Zh. Eksp. Teor. Fiz. **37** (1959) 833.
 - [3] W. E. Lawrence and S. Doniach: in Proc. 12th Int. Conf. Low Temp. Phys. Kyoto, 1970, edited by E. Kanda (Academic Press of Japan, Kyoto, 1971), p.361
 - [4] R. A. Klemm, M. R. Beasley and A. Luther: J. Low Temp. Phys. **16**, (1974) 607.
 - [5] L. N. Bulaevskii and A. A. Guseinov: JETP Lett. **19** (1974) 382.
 - [6] A. G. Lebed and K. Yamaji: Phys. Rev. Lett. **70** (1998) 2697.
 - [7] M. Miyazaki, K. Kishigi and Y. Hasegawa: J. Phys. Soc. Jpn. **67** (1998) 2618.
 - [8] for a review, T. Ishiguro and K. Yamaji: *Organic Superconductors*
 - [9] Y. Yoshida, R. Settai, Y. Onuki, H. Takei, K. Betsuyaku and H. Harima: J. Phys. Soc. Jpn. **67** (1998) 1677.
 - [10] A. G. Lebed: Pis'ma Zh. Eksp. Teor. Fiz. **44** (1986) 89; translation: JETP Lett. **44** (1986) 114.
 - [11] N. Dupuis, G. Montambaux and C. A. R. Sá de Melo: Phys. Rev. Lett. **70** (1993) 2613.

- [12] N. Dupuis and G. Montambaux: Phys. Rev. **B 49** (1994) 8993.
- [13] Y. Hasegawa and M. Miyazaki: J. Phys. Soc. Jpn. **65** (1996) 1028.
- [14] M. Miyazaki and Y. Hasegawa: J. Phys. Soc. Jpn. **65** (1996) 3238.
- [15] K. Kanoda and K. Miyagawa: Phys. Rev. **B 54** (1996) 76.
- [16] Y. Nakazawa and K. Kanoda: Phys. Rev. **B 55** (1997) 8670.
- [17] S. M. De soto et al.: Phys. Rev. **B 52** (1995) 103641.
- [18] H. Mayaffre et al.: Phys. Rev. Lett. **75** (1995) 4122.
- [19] T. M. Rice and M. Sigrist: J. Phys. Condens. Matter **7** (1995) L643.
- [20] K. Ishida, Y. Kitaoka, K. Asayama, S. Ikeda, S. Nishizaki and T. Fujita: Phys. Rev **B 56** (1997) 505.
- [21] K. Ishida et al.: Nature. **396** (1998) 658.
- [22] S. Nishizaki, Y. Maeno, S. Farner, S. Ikeda and T. Fujita: Physica C **282-287** (1997) 1413.
- [23] D. F. Agterberg: Phys. Rev. Lett. **80** (1998) 5184.
- [24] D. R. Hofstadter: Phys. Rev. **B 14** (1976) 2239.